Agricultural Water Management 252 (2021) 106929

Contents lists available at ScienceDirect

Agricultural Water Management

journal homepage: www.elsevier.com/locate/agwat

Performance of the CSM-CROPGRO-soybean in simulating soybean growth and development and the soil water balance for a tropical environment

Evandro Henrique Figueiredo Moura da Silva[a,b,*], Kenneth J. Boote[b], Gerrit Hoogenboom[b,c], Alexandre Ortega Gonçalves[d,e], Aderson Soares Andrade Junior[f], Fabio Ricardo Marin[a]

[a] Luiz de Queiroz College of Agriculture, University of São Paulo, Piracicaba, SP, Brazil
[b] Department of Agricultural and Biological Engineering, University of Florida, Gainesville, FL, USA
[c] Institute for Sustainable Food Systems, University of Florida, Gainesville, FL, USA
[d] Brazilian Agricultural Research Corporation, Soils, Rio de Janeiro, RJ, Brazil
[e] Brazilian Agricultural Research Corporation, Environment, Jaguariúna, SP, Brazil
[f] Brazilian Agricultural Research Corporation, Mid-North, Teresina, PI, Brazil

ARTICLE INFO

Handiling editor: Dr Z Xiying

Keywords:
Soil management practices
Modelling
Irrigated agriculture
Drought stress
Soil moisture
DSSAT

ABSTRACT

Continuous monitoring of soil water content is a crucial element for sustainable agricultural water management. The goal of this study was to use the Cropping System Model (CSM)-CROPGRO-Soybean model in conjunction with field data to determine the impact of different irrigation regimes, soil texture, and tillage practices on soybean [*Glycine max* (L.) Merr.] growth, development, and yield for tropical conditions. Field experiments were conducted at two sites: (i) Piracicaba with conventional tillage (PI-1, season 2016–2017), and no-tillage practices (PI-2, season 2017–2018), where the experiments were irrigated with full water requirements; and (ii) Teresina under conventional tillage (season 2019) with two irrigation treatments of full (TE-1) and 50% (TE-2) water requirements. Soil water content was measured for all experiments using an electromagnetic probe installed at several depths. The results showed that the model was able to simulate soybean growth and development for the different sites, with a very good agreement (D-statistic > 0.8) between the simulated and observed data. In addition, the soil water content was simulated with satisfactory accuracy (D-statistic > 0.5). Following model evaluation, long-term hypothetical scenarios for different soil tillage practices and water management regimes were simulated for Piracicaba and Teresina sites. The results showed that the use of no-tillage could reduce the average amount of irrigation in Piracicaba by 30% and in Teresina by 17%, achieving the same yield level as conventional tillage. Thus, the CSM-CROPGRO-Soybean can be used as a tool for determining optimum water management practices for tropical environments.

1. Introduction

Brazil is an important tropical agricultural region and is the second-largest soybean [*Glycine max* (L.) Merr.] producer in the world. In a tropical environment, periods of drought during the rainy season or during the second cropping cycle (sowing at the end of the rainy season) are considered the most limiting factors for crop yield (Battisti et al., 2018; Multsch et al., 2020). This happens because most tropical rainfall is characterized by irregularity and high intensity, while crop water needs are generally large due to high temperatures and strong solar radiation (Nieuwolt, 1989). Therefore, improved water management is an important component for increasing agricultural sustainable intensification in tropical environments.

Evaluating the soil-crop water balance is a proven approach for understanding drought stress effects during the growing season (Brisson et al., 1992; Ritchie, 1998; Candogan et al., 2013; Zhou and Zhi Zhao, 2019). Process-based crop models are useful tools for simulating the soil water balance, plant growth, and development, for quantifying crop yield, and for exploring alternate options for water management (Alagarswamy et al., 2000; Sau et al., 2004; Soldevilla-Martinez et al., 2014; Battisti and Sentelhas, 2017). The soil water balance can estimate the amount of water available for root uptake along with water loss quantification (evaporation and drainage), which are important to design effective management strategies for soil water conservation

* Corresponding author at: Luiz de Queiroz College of Agriculture, University of São Paulo, Piracicaba, SP, Brazil.
E-mail address: ehfmsilva@usp.br (E. Henrique Figueiredo Moura da Silva).

https://doi.org/10.1016/j.agwat.2021.106929
Received 24 December 2020; Received in revised form 8 March 2021; Accepted 11 April 2021

Table 1
Description of field experiments conducted in Piracicaba (PI-1 and PI-2) and Teresina (TE-1 and TE-2), Brazil.

Experiment	Crop season	Cultivar	Effective irrigation (mm)	Tillage practices	Sowing date	Harvest date	Plant density (plants/m^2)
PI-1	2016/2017	BRS399	177.6	Conventional tillage	Nov 14	Mar 9	35.5
PI-2	2017/2018	BRS399	242.4	No-tillage	Dec 16	Apr 5	35.5
TE-1	2019	8579RSF	418.3	Conventional tillage	Jul 26	Oct 21	22.0
TE-2	2019	8579RSF	271.6	Conventional tillage	Jul 26	Oct 21	22.0

(Hoogenboom et al., 1991; Heinemann et al., 2000, Nijbroek et al., 2003).

Field data can be used in conjunction with model simulations for specific environments to achieve a better understanding of the processes that control the soil water balance and to explore alternatives for long-term water management. The CROPGRO model (Boote et al., 1998) is one of the more robust and widely disseminated crop models in the world and is part of the Decision Support System for Agrotechnology Transfer (DSSAT) (Jones et al., 2003; Hoogenboom et al., 2019a, Hoogenboom et al., 2019b). The CROPGRO-Soybean model simulates soybean growth across a wide range of environmental and management conditions. Soil water movement is simulated using a tipping bucket (Ritchie, 1998) and the United States Department of Agriculture (USDA) SCS curve number approach (Williams, 1991) to represent soil water redistribution, infiltration, and runoff. The time step for soil water balance is daily, and the model considers root water uptake from each individual soil horizon or layer (homogeneous horizontally), and drainage of water through the profile and below the root zone (Boote et al., 2008). The functional soil water balance model used in CROPGRO requires inputs for soil water holding characteristics: (i) permanent wilting point or lower limit of plant extractable soil water (LL), (ii) field capacity or drained upper limit (DUL), and (iii) field saturation or saturated soil water content (SAT) (Ritchie, 1998). The soil water holding traits can be estimated using the SBUILD tool available in the DSSAT software (Hoogenboom et al., 2019b), based on soil texture, bulk density, and organic carbon content data, as well as soil surface and general soil profile characteristics.

Soil water content is an essential variable for evaluating the soil water balance and is very important for water management of cropping systems. An accurate estimate of the soil water balance can help with improving water use efficiency (Qubaja et al., 2020), sustainable crop intensification (Rosa et al., 2017), and irrigation efficiency (Nijbroek, 2003; Valentín et al., 2020); and should be tested with a robust set of experimental data. We are unaware of any published reports that have evaluated the soil water balance and associated crop growth and development with the CSM-CROPGRO-Soybean model with experimental data from tropical environments. The objectives of this study were, therefore, to calibrate and evaluate the performance of the CSM-CROPGRO-Soybean model for simulating soybean growth and development and especially soil moisture content; and to apply hypothetical scenarios using different water management and conservation tillage options for two tropical environments.

2. Materials and methods

2.1. Field experiments

Irrigation experiments were conducted in Piracicaba (22°43′S, 47°38′W, 524 m a.s.l), São Paulo, southeast Brazil, during the 2016/2017 growing season (PI-1) and 2017/2018 growing season (PI-2); and in Teresina (05°05′S, 42°48′W, 74 m a.s.l), Piaui, northern Brazil, during the 2019 growing season. The climate classification for Piracicaba is Cwa (high-altitude tropical climate) and for Teresina is Aw (tropical savanna climate) (Köppen, 1931). Daily weather data for Piracicaba were obtained from the Luiz de Queiroz College of Agriculture (ESALQ) on-site automatic weather station, University of São Paulo (http://www.leb.esalq.usp.br/posto/) (Supplementary Material - Fig. S1 and S2), and for Teresina were obtained from the Teresina-A312 on-site automatic weather station managed by *Instituto Nacional de Meteorologia* (INMET) (http://www.inmet.gov.br/portal/index.php?r = estacoes/estacoes Automaticas) (Supplementary Material - Fig. S3). For both automatic weather stations, the following daily variables were measured: (i) total solar radiation (MJ/m^2/day); (ii) maximum and minimum air temperatures (ºC); and (iii) rainfall (mm).

Fields were cropped with soybean BRS399, a maturity group (MG) 6.0 cultivar with an indeterminate growth habit in Piracicaba; and 8579RSF, a MG 8.0 cultivar with an indeterminate growth habit in Teresina (Table 1). The seeds were inoculated with *Bradyrhizobium elkanii* (strains SEMIA 587 and SEMIA 5019) at a concentration of 5 × 10^9 CFU/mL (colony forming units). Fertilization management was performed according to pre-established applications based on phenological stages (Fehr and Caviness, 1977) and soil analysis (see Supplementary Material – Tables S1 and S2). Pesticide management was performed with the goal of minimizing potential damage due to pests and diseases through weekly monitoring of the crop for pests and diseases to evaluate the effectiveness of pest control (see Supplementary Material – Table S3).

The experiments in Piracicaba were conducted with full water requirements on a Eutric Rhodic Ferralic Nitisol soil under conventional tillage for PI-1, with subsoiling (0.45 m deep) and grid leveling operations, and no-tillage practices for PI-2 sown in wheat crop residue (4000 kg/ha). In Teresina, the experiments were conducted on a Dystrophic Red Yellow Acrisol soil under conventional tillage, with subsoiling (0.45 m deep) and grid leveling operations, and two irrigation treatments: full (TE-1) and 50% (TE-2) of full water requirements (Table 1). The Piracicaba experiments were irrigated by center pivot sprinklers Senninger Model i-Wob-UP3, while at Teresina a sprinkler line-source technique, sprinklers Fabrimar Model A232, was used.

The irrigation amounts were scheduled by potential evapotranspiration (ETo) that was determined for both sites with the Priestley-Taylor (PT) method (Priestley and Taylor, 1972) based on solar radiation and air temperature variables that were recorded with sensors that were properly calibrated and with weather data that were checked daily at the on-site weather station. The PT method was applied under minimum advection conditions (see Supplementary Material – Fig. S4), using empirical parameter $\alpha = 1.26$ (Pereira and Nova, 1992). The PT method showed a close performance when compared to the Penman-Monteith method for Piracicaba (Villa Nova and Pereira, 2006) and Teresina (Andrade Junior et al., 2018). Subsequently, crop evapotranspiration was computed by multiplying ETo by the crop coefficient (Kc) as described in FAO-56 (Allen, 1998). Irrigation was triggered when the available water in the top 0.2 m of the soil profile dropped below 80%, the irrigation schedule was: (i) 277 mm for the total amount of irrigation applied with, on average, 21 mm per irrigation application and total of 12 irrigation application during the season for PI-1; (ii) 378 mm for the total amount of irrigation applied with, on average, 25 mm per irrigation application and total of 13 irrigation application during the season for PI-2; (iii) 529 mm for the total amount of irrigation applied with, on average, 14 mm per irrigation application and total of 38 irrigation application during the season for TE-1; and (iv) 366 mm for the total

Table 2
Original and calibrated parameters for the Eutric Rhodic Ferralic Nitisol soil profile from Piracicaba and the Dystrophic Red Yellow Acrisol soil profile from Teresina.

Site	Depth (m)	Bulk Density (g/cm^{-1})	Clay (%)	Silt	Original soil: SRGF[a]	Original soil: Lower limit (cm^3/cm^3)	Original soil: Drained upper limit	Original soil: Saturated upper limit	Calibrated soil: SRGF	Calibrated soil: Lower limit (cm^3/cm^3)	Calibrated soil: Drained upper limit	Calibrated soil: Saturated upper limit
Piracicaba	0.1	1.31	46	21	1.000	0.257	0.383	0.442	1.000	0.235	0.363	0.508
	0.2	1.31	46	21	0.821	0.257	0.383	0.442	1.000	0.235	0.363	0.508
	0.3	1.31	46	21	0.689	0.257	0.383	0.442	0.800	0.235	0.342	0.508
	0.4	1.32	57	18	0.549	0.325	0.452	0.460	0.800	0.264	0.432	0.534
	0.5	1.32	57	18	0.459	0.325	0.452	0.460	0.600	0.264	0.432	0.534
	0.6	1.35	56	19	0.368	0.324	0.452	0.460	0.500	0.304	0.432	0.520
	1.2	1.35	56	19	0.135	0.324	0.452	0.460	0.300	0.304	0.432	0.520
	1.5	1.37	53	20	0.058	0.303	0.432	0.456	0.080	0.283	0.422	0.526
Teresina	0.1	1.51	11	20	1.000	0.062	0.162	0.405	1.000	0.081	0.173	0.355
	0.2	1.51	11	20	1.000	0.062	0.162	0.405	1.000	0.081	0.173	0.368
	0.3	1.51	11	20	0.607	0.062	0.162	0.405	0.900	0.081	0.183	0.368
	0.4	1.49	26	26	0.497	0.122	0.239	0.413	0.800	0.090	0.183	0.370
	0.5	1.49	26	26	0.407	0.122	0.239	0.413	0.700	0.090	0.193	0.370
	0.6	1.49	26	26	0.333	0.122	0.239	0.413	0.600	0.080	0.193	0.370
	1.2	1.49	26	26	0.165	0.118	0.232	0.413	0.200	0.080	0.193	0.370
	1.5	1.5	25	24	0.067	0.118	0.232	0.413	0.080	0.070	0.203	0.370
	1.8	1.5	25	24	0.037	0.118	0.232	0.413	0.080	0.070	0.203	0.370

[a] Soil root growth factor. The fractional hospitality of soil to root length growth in each soil layer (Marin et al., 2011).

amount of irrigation applied with, on average, 10 mm per irrigation application and total of 38 irrigation application during the season for TE-2 (see irrigation events in Supplementary Material – Fig. S5). The irrigation management strategy that was adopted in this study could have overestimated water consumption; according to Silva et al. (2019) the use of Kc can overestimate crop evapotranspiration by up to 20% for tropical environment.

Field observations and measurements for each experiment included daily phenology observations with recorded dates of emergence, beginning flowering (R1), beginning pod (R3), beginning seed (R5), and physiological maturity (R7) defined as when 50% of the plants reached that particular stage (Fehr and Caviness, 1977). Leaf area index (LAI), was measured using the plant canopy analyzer LI-COR Model LAI-2200C and following the recommendations proposed by Gonçalves et al. (2020). Biomass samples were collected at approximately 10-day intervals from 1-m of row with a row spacing of 0.5 m, from each of four replications. The total plot size per replicate was 54 m^2. Biomass was separated into leaf dry matter, stem dry matter, total top dry matter, and grain weight, and the individual samples were weighed after oven drying to constant weight at 70 ± 5 ºC. At final harvest, crop yield was collected from three center rows (9 m^2) from each replication. LAI measurements were conducted at approximate 10-day intervals between V3 and R7 with four replications.

Volumetric soil water content measurements were made using an electromagnetic probe that had previously been calibrated according to Topp et al. (1980) [Decagon Devices Model GS3 (PI-1 and PI-2), and a Campbell Scientific Model CS650 probe (TE-1 and TE-2)] at 30-min time intervals and then converted to a daily value. The electromagnetic probe was installed in the center of the irrigated area, with the sensors installed both in the row and between the rows, at an average depth of 0.20 m (0.18–0.23 m) and 0.50 m (0.48–0.53 m) in Piracicaba, and at 0.20 m (0.18–0.23 m), 0.30 m (0.28–0.33 m) and 0.40 m (0.38–0.43 m) in Teresina; both sites had four replications for each depth. The measurements were initiated at 13 days after sowing (DAS) for a total of 104 observations for PI-1, and at 8 DAS for a total of 91 daily observations in PI-2. TE-1 and TE-2 measurements were started at 31 DAS for a total of 32 observations for each experiment.

2.2. *Crop model*

The CSM-CROPGRO-Soybean model v.4.7.5 (Jones et al., 2003; Hoogenboom et al., 2019a; Hoogenboom et al., 2019b) simulates growth, development, yield, and soil water content during the crop season using a modular crop model structure described by Jones et al. (2001). The model computes the hourly distribution of temperatures (see Parton and Logan, 1981; Kimball and Bellamy, 1986), solar radiation, and photosynthesis photon flux density, considering photosynthetic irradiance split into direct and diffuse components (see Erbs et al., 1982; Spitters, 1986; Spitters et al., 1986). The hourly canopy photosynthesis simulations are is integrated to a daily photosynthesis value following the light interception and leaf to canopy assimilation method described by Boote and Pickering (1994), Boote et al. (1998). Growth and maintenance respiration depend on temperature, crop photosynthesis rate, and current crop biomass (see Wilkerson et al., 1983; Jones et al., 1989); phenological development is calculated using linear-plateau functions that describe soybean cultivars sensitivity to both photoperiod and temperature (see Grimm et al.,1993; Grimm et al., 1994; Boote et al., 2021).

The model computes evapotranspiration using two different approaches: the Priestley-Taylor method (Priestley and Taylor, 1972), which is the default option, and the FAO-56 Penman-Monteith method (Allen et al., 1998). Potential transpiration, *i.e.*, crop water demand, is computed as the product of the potential (reference) evapotranspiration of either ET method and a model-computed crop coefficient that depends on daily leaf area index (LAI). The DSSAT approach for crop models uses an asymptotic function for daily LAI to compute a dynamic crop coefficient, with solar energy extinction equal to 0.68 (Sau et al., 2004, Boote et al., 2008). This coefficient partitions reference evapotranspiration to either soil water evaporation or crop transpiration based on a crop energy extinction coefficient as described by Sau et al. (2004) and Boote et al. (2008). The soil water evaporation can be calculated by two methods in DSSAT: the Suleiman–Ritchie method is currently the default option (Suleiman and Ritchie, 2003), while the Ritchie Two Stage method (Ritchie, 1972) is an older version that was previously used in DSSAT.

The soil water balance simulates the daily processes that directly affect soil water content: rainfall, irrigation, plant transpiration, soil water evaporation, infiltration, runoff, and drainage (Porter et al., 2004). Infiltration is calculated as the difference between water entry (rainfall and/or irrigation); and surface runoff, calculated using the USDA runoff curve number approach (Williams, 1991). Downward flow controls the rate of water movement between layers with a tipping bucket concept, using a drainage coefficient that is defined for the entire soil profile. Thus, drainage from one layer to the next occurs when soil water content exceeds the field-capacity water holding capacity in each layer. Potential root water uptake is a function of root length density and fraction available soil water content in each soil layer and is integrated over all soil layers where roots are present (Boote et al., 2008). Actual root water uptake is the minimum of potential root water uptake and potential transpiration (water) demand. Under soil water limitations when potential root water uptake is less than the transpirational demand, both photosynthesis (growth) and transpiration are reduced by a ratio, *i.e.*, the actual daily root water uptake divided by the daily transpirational demand.

To evaluate the accuracy of CSM-CROPGRO-Soybean model for the R1, R3, R5 and R7 development stages, the predictions were compared with the observed data. Also, the response of the model was analyzed for LAI, leaf and stem dry matter, total tops dry matter, grain weight, and for soil water content for different soil layers where measurements were taken as described previously.

The simulations were conducted using the Priestley-Taylor potential evapotranspiration method (Priestley and Taylor, 1972), the Suleiman–Ritchie soil water evaporation method (Suleiman and Ritchie, 2003); and the Century soil organic matter method (Parton et al., 1992; Gijsman et al., 2002). As soil water content measurements were started in V3 stage (Fehr and Caviness, 1977), we set the initial soil moisture to 50% of available soil water to initiate the soil water simulations of the model at 30 days prior to sowing.

The soil profiles data were created using the soil granulometry (texture) obtained on site by Gimenes (2016) for Piracicaba (PI-1 and PI-2) and by Melo et al. (2014) for Teresina (TE-1 and TE-2). The soil water holding characteristics including LL, DUL, and SAT for each soil layer as well as bulk density and drainage rate were computed with the SBUILD program of DSSAT (Uryasev et al., 2004), which uses a pedo-transfer function to convert soil texture into soil water holding traits (Table 2). For both soils, these initial soil water-holding traits were subsequently calibrated following four steps: (i) the first step was simulating the soil water content for different depths and adjusting the LL and SAT traits; (ii) step 2, adjusting only DUL; (iii) step 3, adjusting only the soil root growth factor (SRGF); (iv) step 4, re-calibration of LL, DUL, and SAT. The calibration procedures for all steps were conducted by a trial-and-error method against observed soil water content values, using data set from PI-1 for Piracicaba and from TE-1 for Teresina to improve on the statistics computed with the graphics program. Subsequently the soil water content was evaluated using data set from PI-2 for Piracicaba and from TE-2 for Teresina.

We also simulated daily soil water evaporation, root water uptake (equivalent to crop transpiration), extractable water, cumulative runoff, drainage, and mulch evaporation to analyze the water balance performance simulated by the model. For the soil water content, we simulated the 0.20 m (0.15–0.20 m) and 0.50 m (0.40–0.50 m) soil depths for Piracicaba, and the 0.20 (0.15–0.20 m), 0.30 (0.20–0.30 m), and 0.40 m (0.30–0.40) soil depths for Teresina. Although the root length and depth were not measured in this study, the soil depths were chosen to represent a typical root system of soybean for tropical conditions, which has a higher root density in the top layers from 0.10 to 0.50 m and with a maximum depth of around 0.60 m for typical Brazilian soybean fields (Pivetta et al., 2011; Battisti and Sentelhas, 2017; Balbinot Junior et al., 2018). The SRGF in Table 2 describes the fractional hospitality of successive soil layers to root length growth. The daily distribution of root

Table 3
Final values of the calibrated cultivar coefficients for BRS 399 (MG 6.0) and 8579RSF (MG 8.0) with data from the PI-1 experiment in Piracicaba and data from the TE-1 experiment in Teresina.

Traits	Definition	Unit	BRS 399	8579RSF
CSDL	Critical Short Day Length below which reproductive development progresses with no daylength effect	hour	12.58	12.07
PPSEN	Slope of the relative response of development to photoperiod	1/hour	0.311	0.001
EM-FL	Time between VE and R1	photothermal days	20.4	19.7
FL-SH	Time between R1 and R3	photothermal days	8.2	9.1
FL-SD	Time between R1 and R5	photothermal days	13.7	14.9
SD-PM	Time between R5 and R7	photothermal days	28.7	32.1
FL-LF	Time between R1 and end of leaf expansion	photothermal days	18.0	34.0
LFMAX	Maximum leaf photosynthesis rate at 30°C, 350 vpm CO_2, and high light	mg $CO_2/m^2/s$	1.03	1.40
SLAVR	Specific leaf area of cultivar under standard growth conditions	cm^2/g	335	400
SIZLF	Maximum size of full leaf (three leaflets)	cm^2	180	190
XFRT	Maximum fraction of daily growth that is partitioned to seed + shell	g/g	1	1
WTPSD	Maximum weight per seed	g	0.19	0.19
SFDUR	Seed filling duration for pod cohort at standard growth conditions	photothermal days	23.0	21.0
SDPDV	Average seed per pod under standard growing conditions	#/pod	2.4	2.3
PODUR	Time required for cultivar to reach final pod load under optimal conditions	photothermal days	10	10
THRSH	Threshing percentage	seed/(seed+shell)	78	77
SDPRO	Fraction protein in seeds	g(protein)/g (seed)	0.4	0.4
SDLIP	Fraction oil in seeds	g(oil)/g(seed)	0.2	0.2

mass to root length in each layer follows the SRGF factor, but is also dependent on the soil water status of each individual soil layer, e.g., root growth is reduced if a soil layer is either too dry or too wet, and whether the rooting front has reached that depth (see Boote et al., 2008). In addition, allocation to root growth ceases when rapid seed growth begins.

The cultivar coefficients for BRS399 (MG 6.0) for Piracicaba and 8579RSF (MG 8.0) for Teresina, were estimated following the procedures developed by Boote (1999), as summarized in three phases: (i) during the first phase, the goal was to evaluate the efficiency of simulations with the default cultivar parameters (M GROUP 6 for BRS399 and M GROUP 8 for 8579RSF) using observed weather, soil, and management; (ii) during the second phase, only the coefficients associated with crop phenology were calibrated, including the following development stages (compared to observed data for R1, R3, R5, and R7); and (iii) during the third phase, the calibration of other crop growth coefficients was also considered, by comparison to measured data on LAI, leaf dry matter, total tops dry matter, and grain weight (Table 3). Specifically, for TE-1, it was necessary to change the PPSEN to mimic the soybean cultivar types grown in low latitude regions, such as northeastern Brazil that has a short-day length to make the cultivar less sensitive to photoperiod. The soybean cultivars recommended for this region were developed to have a very low sensitivity to photoperiod through the use of the long juvenile trait (Campelo et al., 1998; Carpentieri-Pípolo et al. 2002; Viana et al., 2013; Abrahão and Costa, 2018). The calibration of the MG 6.0 was evaluated for PI-2, while the calibration of MG 8.0 cultivar was evaluated for TE-2. For both cultivars, we evaluated the model capacity to predict: (i) phenology, (ii) LAI, (iii) leaf dry matter, (iv) stem dry matter, (v) total tops dry matter, (vi) grain weight, and (vii) soil water content.

2.3. Hypothetical scenarios of water management and conservation tillage

We applied the CSM-CROPGRO-Soybean after calibration and evaluation of the model, to explore water and tillage practices to ask what-if questions (Tsuji et al., 1998; Thornton and Hoogenboom, 1994) by conducting virtual simulation experiments in Piracicaba and Teresina. This included (i) conventional tillage versus no-tillage practices with 4000 kg/ha of crop surface residue in the initial conditions; (ii) rainfed versus irrigation triggered at 30, 40, 50, 60, 70, or 80% water soil available in the 0.30 m of the soil profile, and (iii) irrigation application rates at 10, 20, and 30 mm. For these simulations we used the planting date and initial soil water conditions from the PI-1 experiment for Piracicaba and from the TE-1 experiment for Teresina. The simulations were repeated for 30 seasons using long-term daily historical weather data from 1988 to 2019 for both sites (Supplementary Material - Figs. S6 and S7). The long-term scenarios were evaluated for their response to crop yield, total number of irrigation applications, and the total amount of irrigation applied during the growing season.

2.4. Statistics for model evaluation

The accuracy of simulations was evaluated by comparing daily values of simulations with the observed data from both sites, as described in the previous section. We used the root mean square error (RMSE) (Loague and Green, 1991) and index of agreement (D-statistic) (Willmott et al., 1985) as measures of goodness-of-fit. The values were calculated using the following equations:

$$RMSE = \sqrt{\frac{\sum_{i=1}^{n}(s_i - o_i)}{n}} \quad (1)$$

$$D = 1 - \left[\frac{\sum_{i=1}^{n}(s_i - o_i)^2}{\sum_{i=1}^{n}\left|(s_i - \overline{o}| + |o_i - \overline{o}|\right)^2}\right], \quad 0 \leq D \leq 1 \quad (2)$$

where n is number of observations; s_i is simulated value corresponding to measurement i on each date; o_i is observed value for measurement i; and $\overline{o}$ is the average of observed values (Yang et al., 2014).

The D-statistic and RMSE were used to assess the error associated with simulation in relation to observed data described in the previous session. The D-statistic is the degree to which the observed values are approached by the model simulated values; it ranges from 0 to 1, with 0 indicating no agreement between the observed and predicted values and 1 indicating perfect agreement. Thus, a high value for the D-statistic and a low value for RMSE would imply better performance.

Table 4
Simulated and observed crop phenology for the cultivars BRS399 and 8579RSF after cultivar and soil calibration. Experiments were conducted in Piracicaba, SP during two growing seasons (PI-1 and PI-2) and in Teresina, PI for two water management treatments (TE-1 and TE-2) during one growing season.

Cultivar	Phenology	Observed	Simulated
		day after sowing (DAS)	
Model calibration			
BRS399 (PI-1)	R1, Beginning flowering	39	39
	R3, Beginning pod	54	54
	R5, Beginning seed	64	64
	R7, Physiological maturity	104	104
8579RSF (TE-1)	R1, Beginning flowering	30	30
	R3, Beginning pod	41	41
	R5, Beginning seed	48	48
	R7, Physiological maturity	83	83
Model evaluation			
BRS399 (PI-2)	R1, Beginning flowering	36	36
	R3, Beginning pod	51	49
	R5, Beginning seed	58	57
	R7, Physiological maturity	91	89
8579RSF (TE-2)	R1, Beginning flowering	30	30
	R3, Beginning pod	41	41
	R5, Beginning seed	48	49
	R7, Physiological maturity	83	78

3. Results and discussion

3.1. Simulated phenology, growth and development for BRS-399 and 8579RSF

We used PI-1 and TE-1 treatments for model calibration based on the Priestley-Taylor method for evapotranspiration and the Suleiman-Ritchie method for soil water evaporation. After the second phase of calibration, the model showed a correct prediction of the R1, R3, R5, and R7 for both experiments (Table 4). The PI-2 and TE-2 treatments were then used for evaluation. We observed a good accuracy for the simulation of development for both cultivars BRS-399 and 8579RSF across the phenological stages; the maximum difference between the simulated and the observed values was 5 days.

The evaluation of the CSM-CROPGRO-Soybean model for predicting phenology for TE-2 showed identical results for both simulated and observed R1 and R3, but with the simulated R7 earlier than the observed R7 (Table 4). A shorter simulated cycle (time between planting to physiological maturity) TE-2 than observed for TE-2 is possibly an indication that the real crop did not experience as much drought stress as the simulated crop. There was a reduction in the simulated cycle of TE-2 because the model simulates reproductive development as a function of photoperiod, temperature, and soil water and nitrogen deficits (Boote et al., 1998). In this case, the difference was caused by the prediction of drought stress, which uses the drought stress factor for photosynthesis to account for the effect of a water deficit on the plant physiological processes (Boote et al., 2008), resulting in an acceleration to maturity after R5. This index indicates the daily severity of drought stress during the cropping season and ranges from a value of zero (well-watered conditions) to one (maximum stress) (Fig. 1).

The experiment PI-2 showed identical results for evaluation of R1,

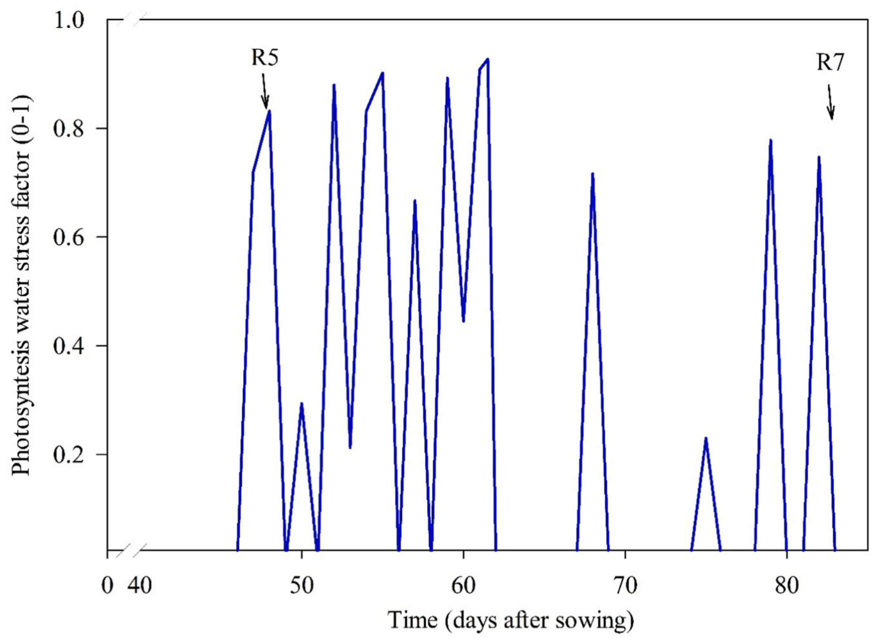

Fig. 1. Simulated photosynthesis drought stress factor during the 2019 season at Teresina (TE-2) after cultivar and soil calibration. Observed phenological stages during the drought period are beginning seed (R5) and physiological maturity (R7).

but was less accurate for the simulation of the R3, R5, and R7 stages. The crop model simulated a slightly shorter cycle than was observed in the field experiment, with a difference between simulated and observed data that ranged from 1 to 2 days between R3 and R7. The model was able to show a similar shortening of the cycle length between PI-1 and PI-2. In PI-2 with a later planting and successively shorter days, flowering and all stages were earlier compared to PI-1. It is possible that day length sensitivity is not sufficiently parameterized (based on the single case of PI-1 with a more normal sowing date). Phenology affects dry matter accumulation and partitioning, ultimately affecting seed yield (Boote et al., 1998; Kim and Schultz, 2020; Salmerón and Purcell, 2016; Soltani and Sinclair, 2012). Thus, the simulated and observed shorter cycle caused the grain yield in PI-2 to be almost 20% lower than PI-1 (Fig. 2). The model successfully simulated this lower yield associated with a shorter duration from planting to physiological maturity due to a later planting.

The full water requirements treatments (PI-1, PI-2, TE-1) did not show any drought stress because the irrigation management was sufficient to supply the evapotranspiration demand throughout the growing season (Fig. 2). In TE-2 periodic drought stresses was simulated between R5 and R7 (Fig. 1) which resulted in a reduction in total crop and grain weight compared to TE-1. Drought during the R5-R7 phase induces a decrease of the grain-filling period by stimulating the acceleration of senescence (Souza, Egli, and Bruening, 1997) (Fig. 1). The water supply for TE-1 resulted in a grain yield of 3290 kg/ha, while for TE-2 the grain yield was 1379 kg/ha; the model was able to successfully simulate a similar response to water deficit with a decrease in total crop weight and grain yield (Fig. 2).

For our calibration procedure for PI-1 and TE-1, we minimized the RMSE, maximized the D-statistic, and visually evaluated whether the cultivar coefficient adjustments were able to provide a better description of the observed growth variables. Based on these indicators, we obtained the best possible adjustment and the calibrated model was able to correctly simulate LAI, leaf dry matter, stem dry matter, total top dry matter, and grain weight over the time compared to the observed data (Table 5). We evaluated the CSM-CROPGRO-Soybean simulations, and found that all evaluated variables were well simulated, with values for the D-statistic that were above 0.90 for all variables, except for the leaf and stem components that had values for the D-statistic that were greater than 0.8 (Table 5).

3.2. Simulation of soil water dynamics

We varied the soil water holding traits from the standard condition (computed via the SBUILD) after cultivar calibration through a trial-and-error method for each soil with the goal to minimize the RMSE and maximize D in order to improve the simulations against the observed soil water content for PI-1 and TE-1. The calibrated soil water holding traits are presented in Table 2. We evaluated the performance of the CSM-CROPGRO-Soybean model to simulate the soil water balance for different depths of the soil profile, and two soil conditions under tropical soybean production systems (Figs. 3, 4). The soil water content in Piracicaba was satisfactorily simulated, as the D-statistic values for both depths, *i.e.*, 0.20 m and 0.50 m, ranged from 0.579 to 0.835 and the values for RMSE ranged from 0.011 to 0.020 cm^3/cm^3. However, there was a tendency of the model to over-estimate soil water content in both experiments (Fig. 3). For the Teresina site, the soil water content was satisfactorily simulated, with values for the D-statistic for the 0.20, 0.30, and 0.50 m soil depths that ranged from 0.535 to 0.984 and values for RMSE that ranged from 0.005 to 0.027 cm^3/cm^3 (Fig. 4); the soil water content was overestimated in TE-1 and underestimated in TE-2. The underestimation of simulated soil water content in TE-2 corroborates with the previous arguments that the model overestimated drought stress (Fig. 1).

The different soil textures at Piracicaba and Teresina resulted in considerable differences in the amount of water retained under no drought stress conditions (PI-1, PI-2, TE-1). We observed a higher soil water content for the soil with the higher clay content, *i.e.*, the soil at Piracicaba, since the clay fraction contributes to the formation of micropores (Dexter, 2004; Zaffar and Sheng-Gao, 2015).

The soil at Piracicaba was a clay loam soil, and showed large soil water content fluctuation for the 0.20 m soil depth, whereas the 0.50 m soil depth had a less variable and higher soil water content, especially at the beginning of the soybean cycle (Fig. 3). The soil water content for the

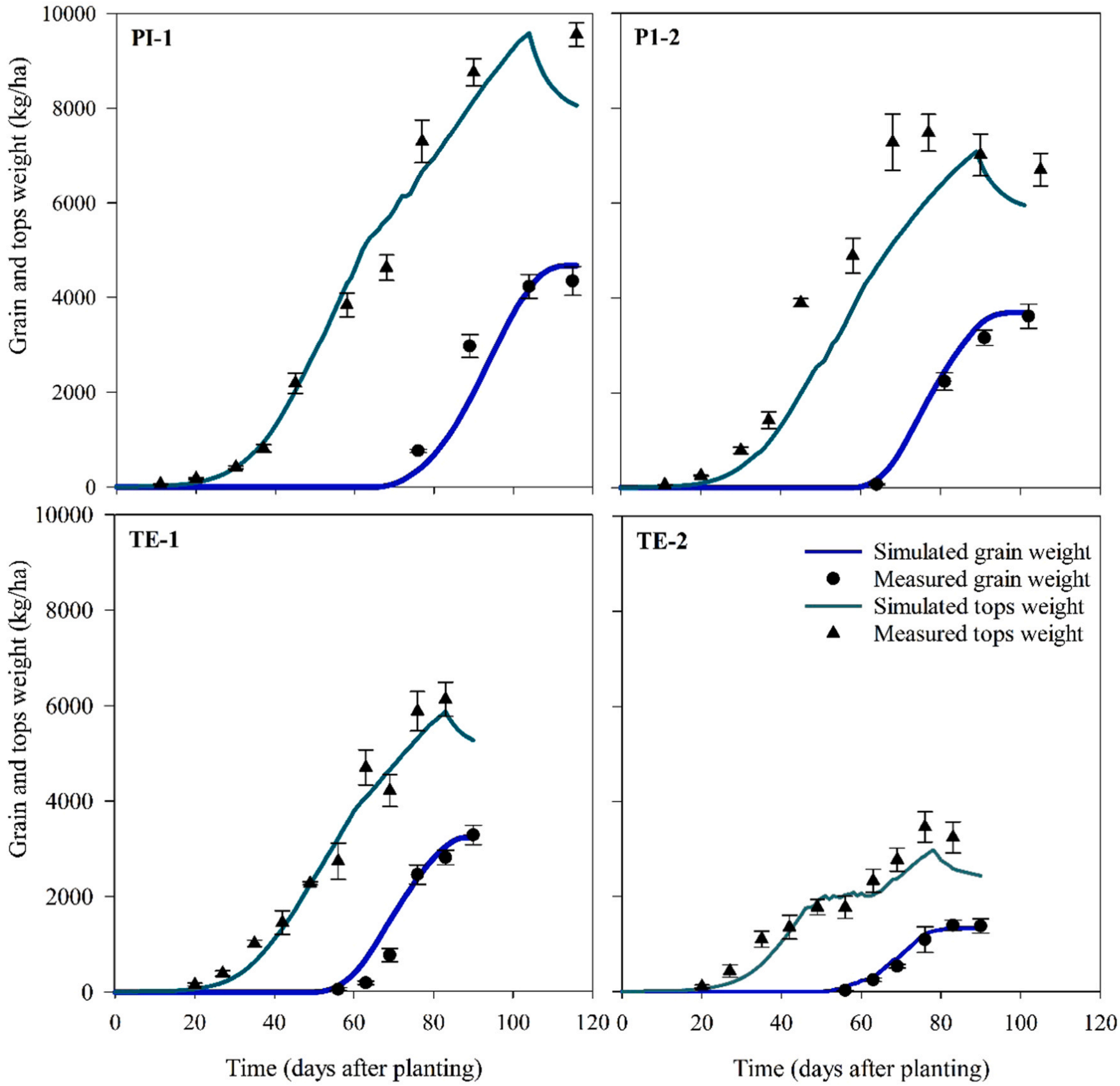

Fig. 2. Simulated and observed grain and total crop (tops) weight and the standard deviation of observed data for the experiments conducted in Piracicaba (PI-1 and PI-2) and Teresina (TE-1and TE-2) after soil and cultivar calibration.

0.50 m depth remained close to the DUL; the model simulated a similar response by smaller amount of soil water extraction by the soybean roots during this phase. The cumulative values for rainfall were 947 mm with 177.6 mm of effective irrigation for PI-1, while PI-2 the rainfall was 703.5 mm with 242.4 mm of effective irrigation.

The soil at Teresina was a sandy loam soil. In both treatments (TE-1 and TE-2) there was a large soil water content oscillation for the 0.20 m soil depth, and a moderate oscillation for the 0.30 and 0.40 m soil depths in TE-1 during the growing season, showing a satisfactory simulated soil water content evaluation for the deeper layers at 60 days after planting (Fig. 4). In TE-2 there was a slow decrease of the soil water content from 40 days after planting for the 0.30 and 0.40 m depths. This could indicate that the roots of the soybeans penetrated more deeply when the surface layers dried out due to soil water evaporation. In these two deeper layers, the soil water content declined and approached LL later during the growing season, which is reflected in a high value for the photosynthesis drought stress factor (Fig. 1) and a reduction in biomass growth and yield for this treatment (Fig. 2).

CSM-CROPGRO-Soybean simulated a large amount of total extractable water in the soil profile during the harvest period in Piracicaba (PI-1 and PI-2) with runoff and drainage values increasing during tropical storms (Fig. 5). For the drought periods between 80 and 100 days after planting in PI-1, which was supplemented with irrigation, the runoff was stabilized and the drainage was less. The cumulative mulch evaporation in PI-2 was computed as described by Porter et al. (2010) and the reduced soil-plus-mulch evaporation allowed the model to simulate the practice of conservation of soil water by maintaining more constant levels of extractable water and a smoother runoff curve. The inclusion of crop residue in the initial conditions of the PI-2 simulation was helpful to improve the statistical indicators for both the evaluation of soil water content and for soybean growth and development.

The experiments in Teresina (TE-1 and TE-2) were conducted under winter conditions, with a high average temperature (28.4 ºC) (Supplementary Material - Fig. S3) and a dry season with only a total of 15.4 mm of rainfall. The irrigation management was responsible for practically all the water requirements of the soybean crop, while the effective irrigation amounts were 418.3 mm for TE-1 and 271.6 mm for TE-2. The model simulated that there was no runoff or drainage during the season, while the cumulative mulch evaporation was less than 5 mm (Fig. 5). This happened because the irrigation management was carried out with a small amount of water per irrigation application. The average irrigation amount was 17.6 mm for TE-1 and 11.7 mm for TE-2, with 2- or 3-

Table 5
Statistical analysis for the time series crop growth variables following cultivar and soil calibration.The experiments were conducted in Piracicaba (PI-1 and PI-2) and Teresina (TE-1 and TE-2).

Treatment	Variable	Unit	RMSE	D-statistic
Model calibration				
BRS399 (PI-1)	Leaf area index	—	0.397	0.983
	Leaf dry matter	kg/ha	120	0.994
	Stem dry matter	kg/ha	485	0.964
	Total tops dry matter	kg/ha	667	0.992
	Grain weight	kg/ha	625	0.960
8579RSF (TE-1)	Leaf area index	—	0.418	0.927
	Leaf dry matter	kg/ha	204	0.874
	Stem dry matter	kg/ha	480	0.819
	Total tops dry matter	kg/ha	394	0.990
	Grain weight	kg/ha	373	0.977
Model evaluation				
BRS399 (PI-2)	Leaf area index	—	0.273	0.984
	Leaf dry matter	kg/ha	392	0.889
	Stem dry matter	kg/ha	495	0.918
	Total tops dry matter	kg/ha	625	0.988
	Grain weight	kg/ha	200	0.994
8579RSF (TE-2)	Leaf area index	—	0.413	0.947
	Leaf dry matter	kg/ha	257	0.823
	Stem dry matter	kg/ha	130	0.954
	Total tops dry matter	kg/ha	385	0.964
	Grain weight	kg/ha	94	0.992

days irrigation intervals. Simulated drainage is calculated by a 'cascading' approach, in which excess water above DUL from an upper layer cascades to lower layers (Ritchie, 1985; Shelia et al., 2018). The soil from Teresina is deeper (1.8 m depth) and we did not observe a soil water content above DUL in the deepest measured layer 0.4 m depth (Fig. 4). Therefore, there was no drainage.

3.3. Simulation of soil water evaporation and root water uptake

PI-1 had a higher soil water evaporation rate during the early stages of the growing season than PI-2 (Fig. 6). The model simulated less soil water evaporation during the PI-2 season because the soil surface water dynamics were modified by the presence of crop residue under no-tillage practices. Other studies also found a satisfactory performance of the CSM model for the simulation of the impact of tillage and residue on soil water dynamics (Andales et al., 2000; Liu et al., 2011; Corbeels et al., 2016; Adhikari et al., 2017). The higher soil water evaporation rate was obtained for PI-1 within the first 20 days after planting, under bare soil conditions with a high soil water content. For the experiments conducted in Piracicaba and Teresina, the soil water evaporation rate decreased during the growing season until rising again near physiological maturity, when the reduction in canopy coverage due to leaf senescence and abscission increased solar radiation to the soil surface and increased soil water evaporation rate (Fig. 6).

The LAI is a very important trait for the simulation of the soil water balance by CSM-CROPGRO-Soybean, because the amount of solar radiation (MJ/m^2) that reaches the soil is a function of LAI, thus impacting soil water evaporation and plant transpiration (Boote et al., 2008; Sau et al., 1999). The root water uptake is calculated using a law of the limiting approach whereby soil water and root resistance, or atmospheric demand control root water uptake (Ritchie, 1981), which depends on the available soil water and root length density of each soil layer or horizon. Potential root water uptake must be computed before actual plant transpiration is computed, featuring an upward flow closely related to soil water evaporation and plant transpiration (Shelia et al., 2018). As expected, we observed a strong relationship between the highest LAI values and the highest root water uptake rates (Fig. 6).

A good calibration of the LAI is relevant to obtain a satisfactory performance for predicting yield (Richetti et al., 2019) and soil water balance simulation. The TE-2 simulation of LAI suggests that the model simulated more drought stress than was observed in the field experiment (Fig. 6), which corroborates with the slightly lower simulated tops and grain weight (Fig. 2) compared with the observed data. The greater severity of the simulated drought stress may explain the 5 day gap (Table 2) in phenological maturity between the simulated and the observed data.

3.4. Simulation of long-term of water management scenarios

Following the evaluation of the CSM-CROPGRO-Soybean model for simulation of soybean growth and development and the soil water balance, we conducted a seasonal analysis based on what-if scenarios for a tropical environment. The long-term simulations for soybean yield and the impact of tillage practices on water management are presented in Fig. 7. The rainfed condition in Piracicaba presented the largest variation in the crop yield among the 30 simulated seasons, and the no-tillage practices increased crop yield by about 240 kg/ha on average (Fig. 7).

The simulations showed that the average yield increased by 564 kg/ha compared to PI-rainfed if irrigation was triggered when 50% available water remained. Among the PI-50 to PI-80 irrigation triggering scenarios, the difference in crop yield was only 50 kg/ha. The use of irrigation made it possible to reduce the production risk in relation to rainfed conditions, because the range between highest and lowest values in PI-rainfed was 3020 kg/ha while the range was 1400 kg/ha for the PI-50 irrigation scenarios. Conservation tillage practices reduced the irrigation amount on average by 43% for PI-30% and 27% for PI-80, while maintaining productivity levels very close to conventional tillage. The use of no-tillage reduced the number of irrigation applications on average by one application among the different scenarios.

The soybean grown in Teresina showed a lower yield potential than in Piracicaba because it was grown in low latitude region during the winter with a shorter life cycle, along with less daily total solar radiation. For the Teresina winter environment with almost no rainfall, the average yield under rainfed conditions was less than 50 kg/ha. Yield response to irrigation was greatest for the first irrigation increments, 0–30, 30–40, or 40–50% triggering thresholds. The highest average crop yield was 3532 kg/ha in TE-70, with 140 kg/ha more yield than TE-60 but required an additional 52 mm in seasonal applied irrigation.

Within a given irrigation scenario such as TE-40, yield was an average of 2084 kg/ha under conventional tillage and 2225 kg/ha with no-tillage practices, while saving 13 mm of water under no-tillage. Surface residue with no-tillage in Teresina resulted in increased yield for triggering supplemental irrigation at 30%, 40%, and 50%, but showed little to no yield benefit at higher triggering levels of 60, 70, or 80% (Fig. 7). However, no-tillage practices reduced the seasonal applied irrigation, on average, by 20 mm for TE-50 and 56 mm for TE-70 (Fig. 7).

The use of a relatively high amount of irrigation per application is common in Brazilian agricultural practices mainly due to a decrease in the energy costs associated with each irrigation event. However, in this case farmers might apply more water than is needed, thus both water and energy are wasted (Kamienski et al., 2019; Marin et al., 2019; Silva et al., 2019). In our findings with DSSAT as a water management tool for scheduling irrigation, decreasing the amount of water per irrigation application from 30 to 10 mm for PI-50 could save 38 mm for conventional tillage and 27 mm for the no-tillage practices. This represents almost 40% of water saved with an increase of three irrigation applications while maintaining the same yield level (Fig. 8). The decreased irrigation application rate from 30 to 10 mm showed the largest reduction in the total amount of water applied for PI-80 with no-tillage practices at around 115 mm. However, as shown in Fig. 7, irrigation triggering above a 50% threshold level in Piracicaba does not result in a

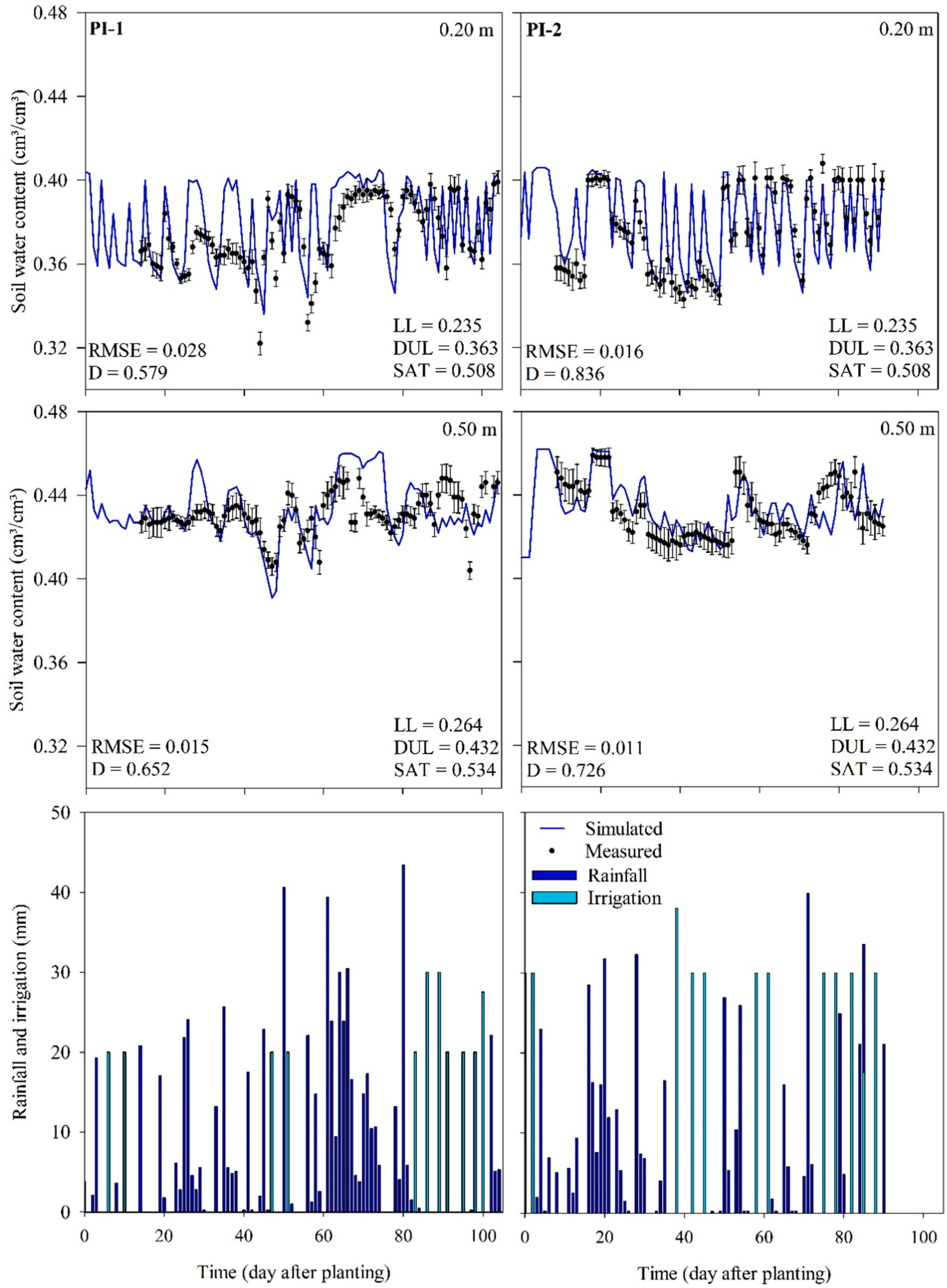

Fig. 3. Simulated and observed soil water content for Piracicaba (PI-1 and PI-2) for the 0.20 and 0.50 m soil depths and the rainfall and irrigation events. The soil water holding characteristics are shown: lower limit of plant extractable soil water (LL), drained upper limit (DUL), and saturated soil water content (SAT).

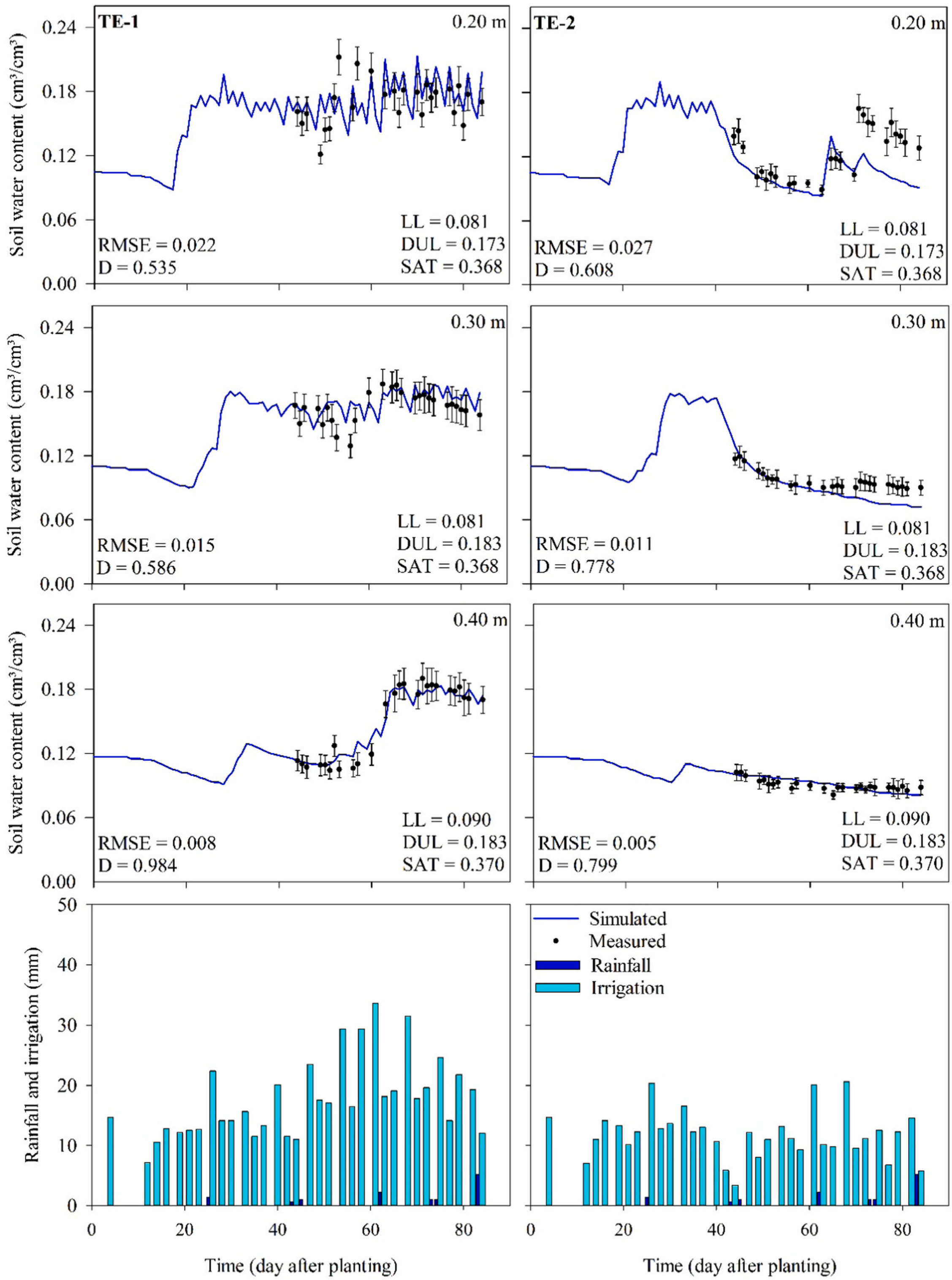

Fig. 4. Simulated and observed soil water content for Teresina (TE-1 and TE-2) for the 0.20, 0.30 and 0.40 m soil depths and the rainfall and irrigation events. The soil water holding characteristics are shown: lower limit of plant extractable soil water (LL), drained upper limit (DUL), and saturated soil water content (SAT).

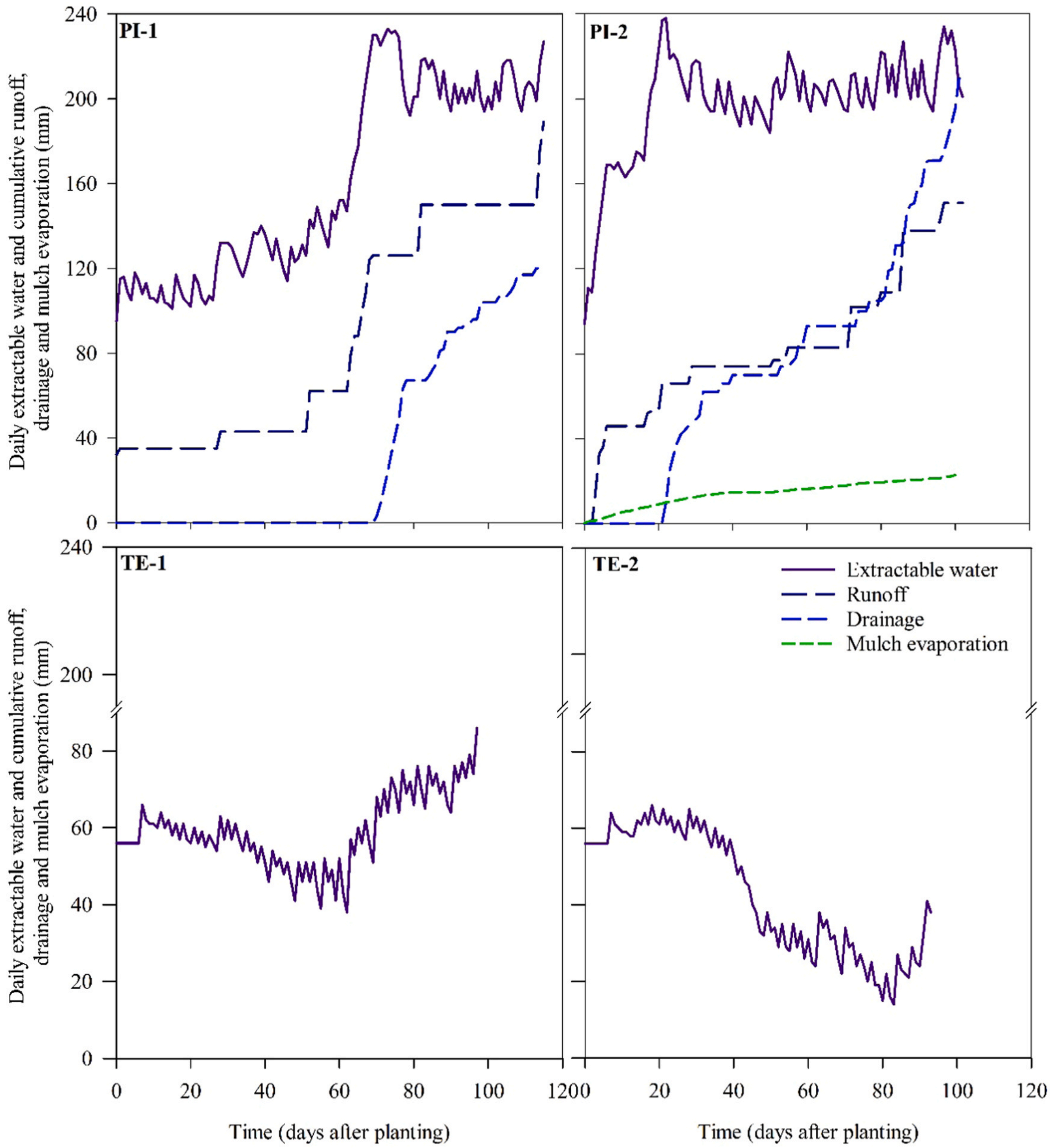

Fig. 5. Simulations for daily extractable water (mm), cumulative runoff, drainage, and mulch evaporation (mm) in the soil profile for experiments conducted in Piracicaba (PI-1 and PI-2), and Teresina (TE-1 and TE-2) after cultivar and soil calibration. The mulch evaporation in PI-1, TE-1, and TE-2 was less than 5 mm (data not shown).

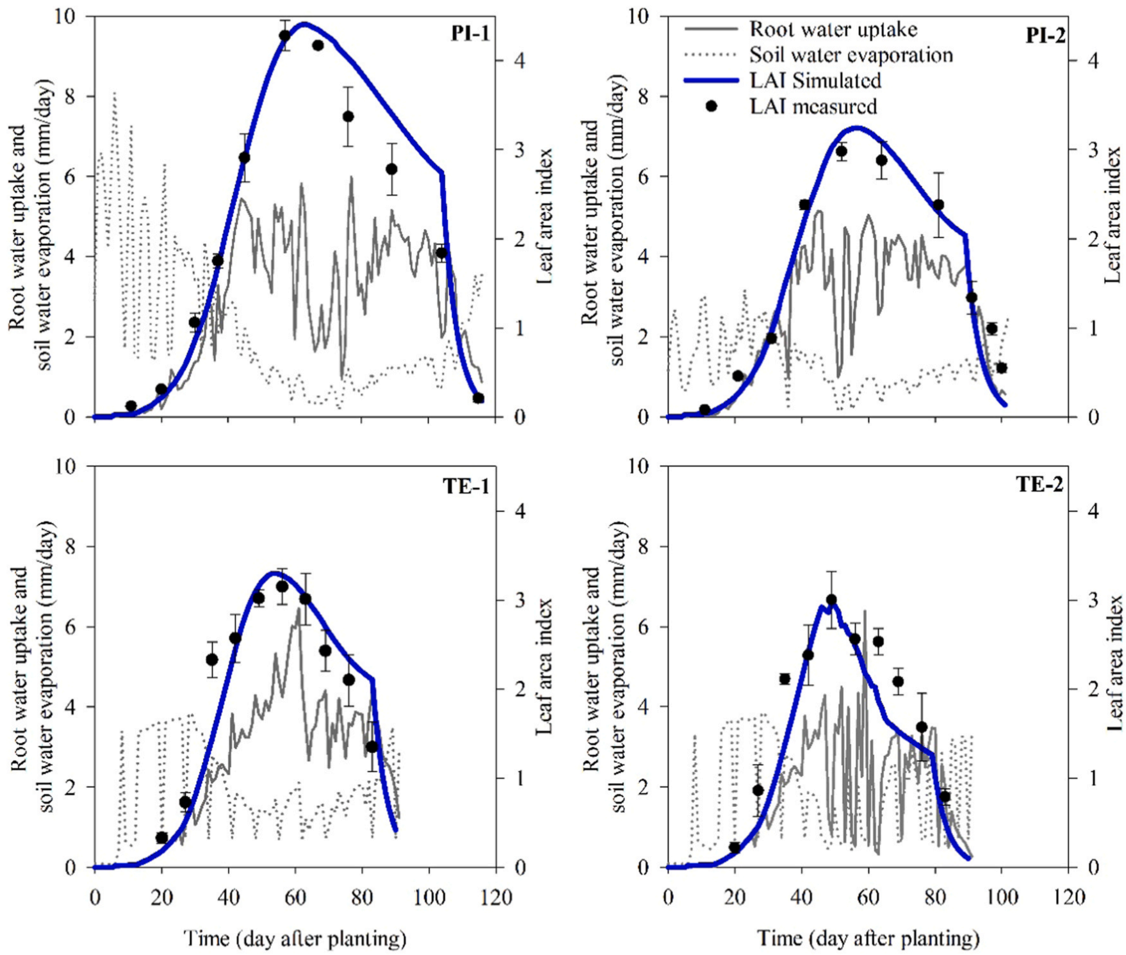

Fig. 6. Simulated and observed leaf area index (LAI; average and standard deviation), and simulated soybean root water uptake and soil water evaporation rate for the experiments conducted in Piracicaba (full crop water requirements, PI-1 and PI-2), and Teresina [TE-1 (full crop water requirements) and TE-2 (50% crop water requirements)] following cultivar and soil calibration.

yield increase despite the increase in water consumption.

The scenarios for Teresina showed that applying irrigation triggered at 60% water remaining is most efficient, showing a greater yield per seasonal applied irrigation (Fig. 7). However, reducing the irrigation amount per application from 30 to 20 mm decreased the total water requirement from 494 to 472 mm with conventional tillage and from 454 to 424 mm with no-tillage practices, at the expense of seven more irrigation applications (Fig. 9). Frequent light irrigations like this may work with drip irrigation, but from a realistic viewpoint, no farmer-producer would apply an irrigation amount of 10 or 20 mm per overhead application to save 20 or 30 mm with an increase in seven applications, so this argument of water-savings is somewhat artificial. Thus, the irrigation management of soybean in Teresina, during the winter with 30 mm of irrigation application rate with no-tillage practices is potentially more appropriate because this site has a deep soil with a good water-retention capacity and a small amount of water loss due to drainage and runoff (Table 2, Fig. 5).

The simulations of the CSM-CROPGRO-Soybean model for both sites showed differences among tillage practices, soil texture, and irrigation amount. As discussed previously, the model was able to explore different scenarios combining tillage practices and water management using long-term historical weather data following successful calibration of the model for crop growth and development and soil moisture. Soil management with the maintenance of soil mulch can contribute to reducing the amount of water required for supplemental irrigation for soybean production and contribute to sustainable intensification of agriculture in Brazil. However, for the agricultural system analysis in the long-term scenarios, it is important to consider that the model showed a slight tendency to overestimate the soil water content under fully irrigated conditions (PI-1, PI-2, TE-1); and to underestimate the soil water content in drought conditions (TE-2). This may suggest the need to improve several model features: 1) the simulated efficiency of applied irrigation that is infiltrating the soil, 2) the soil evaporation method which may cause excessive soil water depletion under drought, and 3) the transpiration method which may also cause too much soil water depletion under drought. Implications for the scenario analyses are that the model at present may over-estimate drought-stress for drought conditions. However, in general the CSM-CROPGRO-Soybean performed very well in this study and demonstrated the potential for using the model as a tool for agricultural water management under tropical conditions.

4. Conclusions

The CSM-CROPGRO-Soybean model of DSSAT was evaluated for its ability to simulate soil water balance and soybean growth and development under a tropical environment. There was a good agreement between simulated and observed soil water content over time under different soils, tillage practices, water requirements, and tropical conditions in Brazil. The long-term scenarios showed that the amount of irrigation for a soybean crop in a tropical environment can be reduced with the use of no-tillage practices. We conclude that the model was able to accurately simulate the soybean growth, development, and yield as

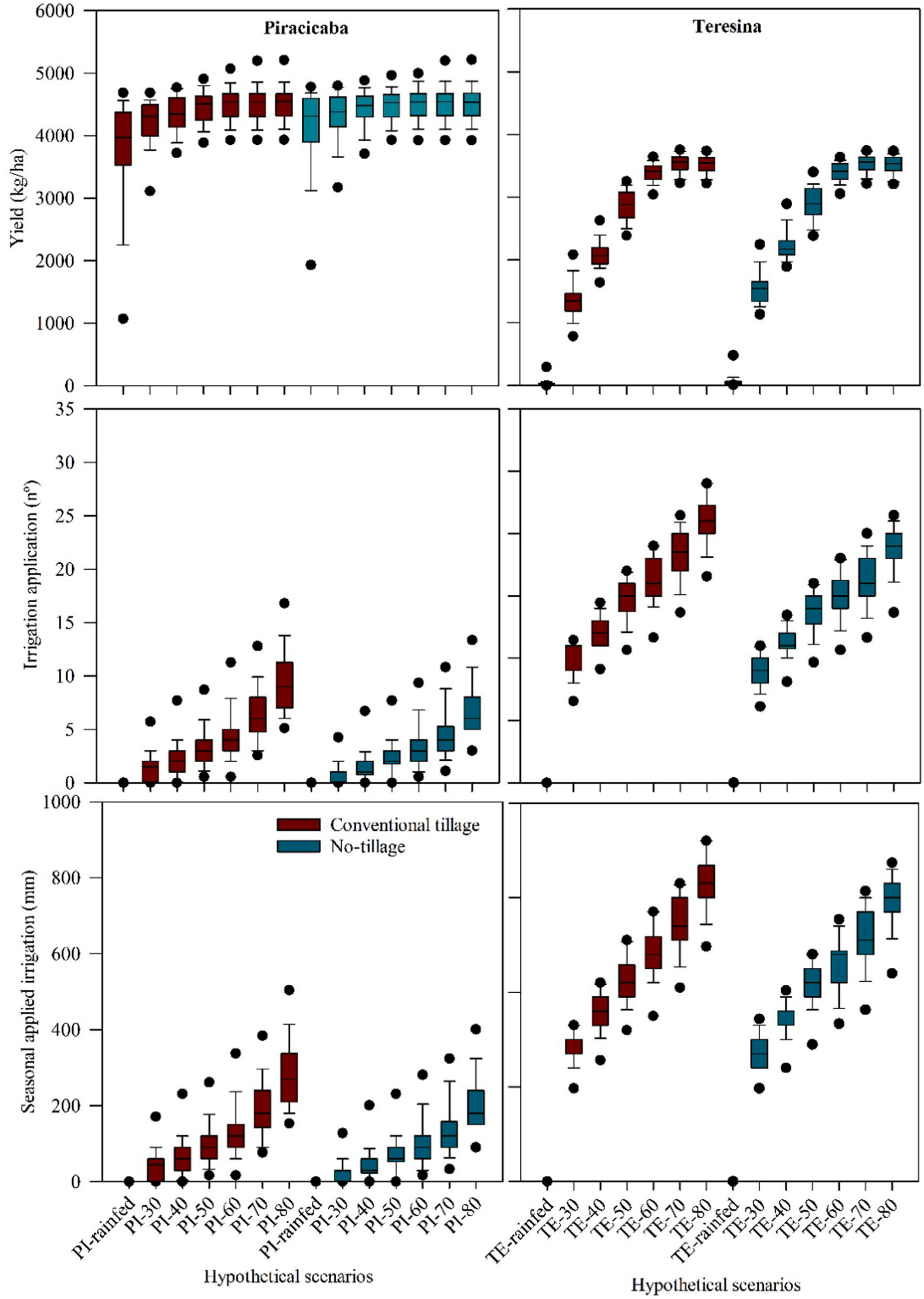

Fig. 7. Simulated long-term scenarios for Piracicaba and for Teresina for rainfed and irrigation management scenarios, triggering irrigation based on 30–80% water remaining in the top 0.30 m of the soil profile for conventional tillage and no-tillage. Boxplots were set at 90th (upper whisker), 75th (upper quartile), 50th (median), 25th (lower quartile), and 10th (lower whisker) percentiles; outliers are shown as black dots.

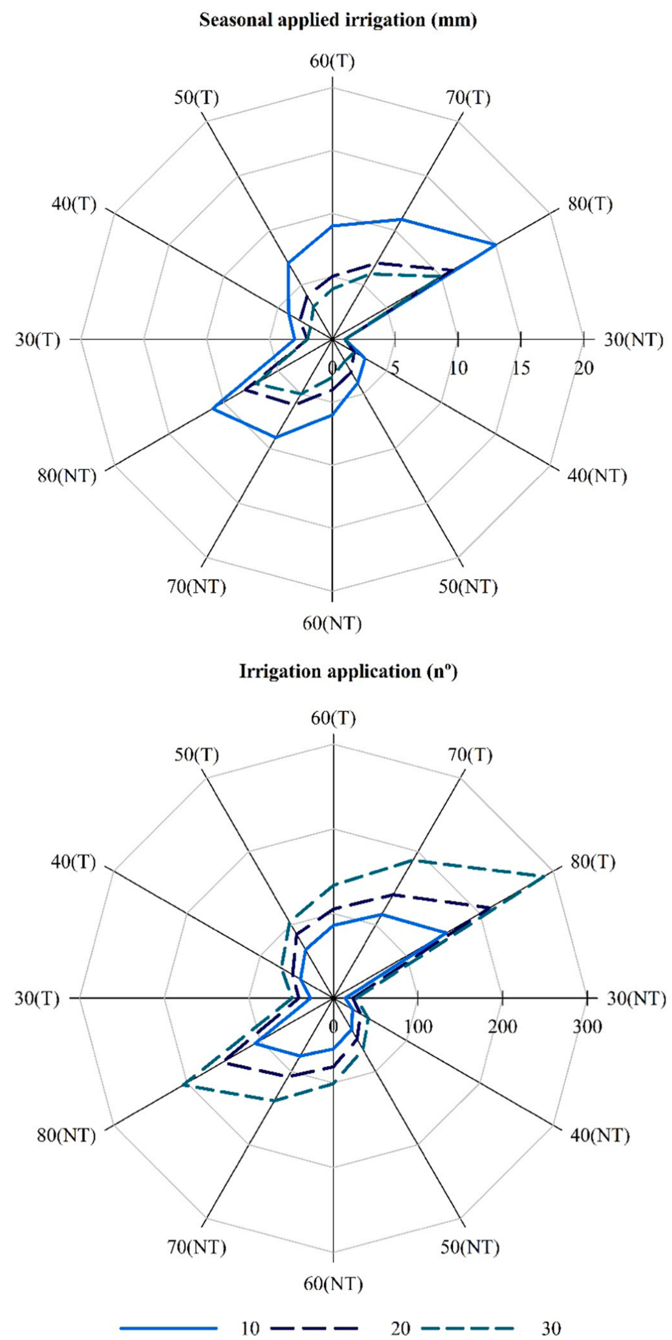

Fig. 8. Total number of irrigation applications and total irrigation applied for the long-term scenarios for Piracicaba under rainfed and irrigated conditions for conventional tillage (T) and no-tillage (NT) and for three application rates, *i. e.* 10 mm, 20 mm and 30 mm, at triggers of 30%, 40%, 50%, 60%, 70%, and 80% of water remaining.

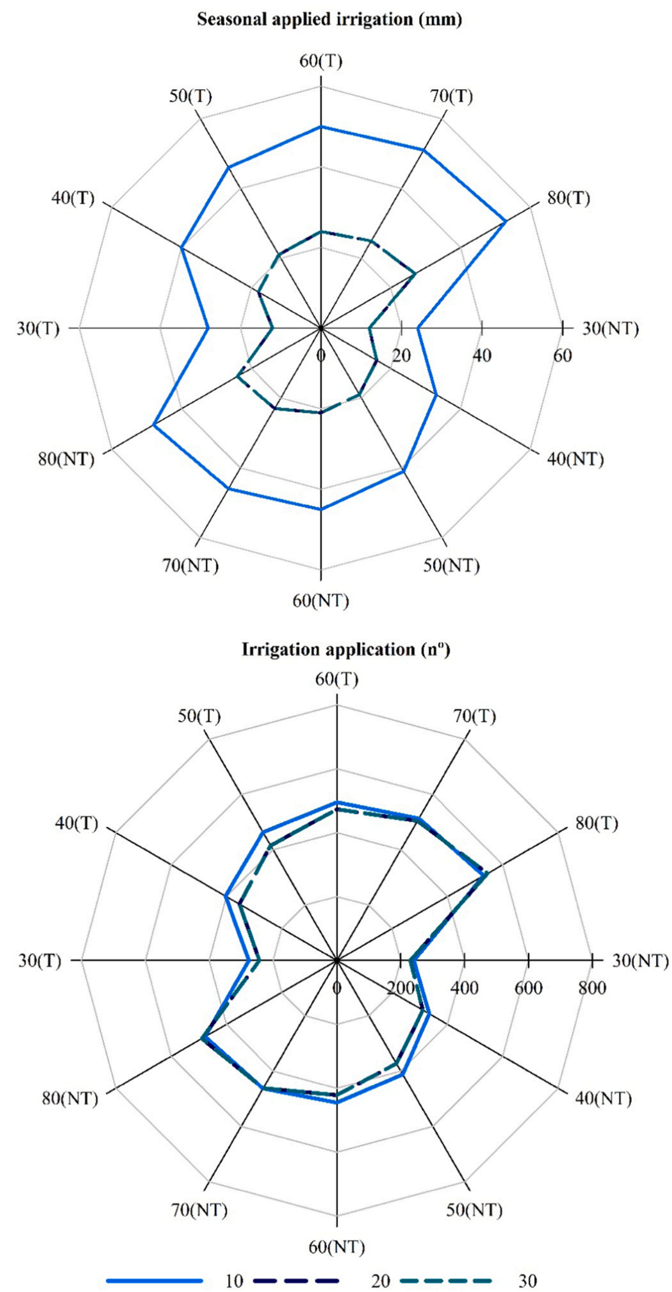

Fig. 9. Total number of irrigation applications and total irrigation applied for the long-term scenarios for Teresina under rainfed and irrigated conditions for conventional tillage (T) and no-tillage (NT) and for three application rates, *i.e.* 10 mm, 20 mm and 30 mm, at triggers of 30%, 40%, 50%, 60%, 70%, and 80% of water remaining.

well as the soil water balance for different tropical environments and that DSSAT can be applied to evaluate different irrigation management options to help conserve water use.

Declaration of Competing Interest

The authors declare that they have no known competing financial interests or personal relationships that could have appeared to influence the work reported in this paper.

Acknowledgments

This research was supported by the Research Foundation of the State of São Paulo (FAPESP 2015/25702-3; 2017/23468-9; 2019/18303-6, 2017/20925-0, 2017/50445-0), Brazilian Research Council (CNPq, 301424/2015-2, 300916/2018-3, 401662/2016-0 and 425174/2018-2), and Coordination for the Improvement of Higher Education Personnel (CAPES)- Ministry of Education of Brazil.

Appendix A. Supporting information

Supplementary data associated with this article can be found in the online version at doi:10.1016/j.agwat.2021.106929.

References

Abrahão, G.M., Costa, M.H., 2018. Evolution of rain and photoperiod limitations on the soybean growing season in Brazil: the rise (and possible fall) of double-cropping systems. Agric. For. Meteorol. 256, 32–45.

Adhikari, P., Omani, N., Ale, S., DeLaune, P.B., Thorp, K.R., Barnes, E.M., Hoogenboom, G., 2017. Simulated effects of winter wheat cover crop on cotton production systems of the Texas rolling plains. Trans. ASABE 60 (6), 2083–2096.

Alagarswamy, G., Singh, P., Hoogenboom, G., Wani, S.P., Pathak, P., Virmani, S.M., 2000. Evaluation and application of the CROPGRO-Soybean simulation model in a Vertic Inceptisol. Agric. Syst. 63 (1), 19–32.

Allen, R.G., Pereira, L.S., Raes, D., Smith, M., 1998. Crop evapotranspiration-Guidelines for computing crop water requirements-FAO Irrigation and drainage paper 56. FAO, Rome.

Andales, A.A., Batchelor, W.D., Anderson, C.E., Farnham, D.E., Whigham, D.K., 2000. Incorporating tillage effects into a soybean model. Agric. Syst. 66 (2), 69–98.

Andrade Junior, A.S., da Silva, C.O., de Sousa, V.F., Ribeiro, V.Q., 2018. Avaliação de métodos para estimativa da evapotranspiração de referência no estado do Piauí. Agrometeoros 25, 1.

Balbinot Junior, A.A., Debiasi, H., Franchini, J.C., Prieto, M.T.M., Moraes, M.T., Werner, F., Ferreira, A.S., 2018. Crescimento e distribuição de raízes de soja em diferentes densidades de plantas. Rev. De. Ciências Agroveterinárias 17 (1), 12–22.

Battisti, R., Sentelhas, P.C., 2017. Improvement of soybean resilience to drought through deep root system in Brazil. Agron. J. 109 (4), 1612–1622.

Battisti, R., Sentelhas, P.C., Parker, P.S., Nendel, C., Gil, M.D.S., Farias, J.R.B., Basso, C. J., 2018. Assessment of crop-management strategies to improve soybean resilience to climate change in Southern Brazil. Crop Pasture Sci. 69 (2), 154–162.

Boote, K.J., 1999. Concepts for calibrating crop growth models. DSSAT Version 3 (4), 179–200.

Boote, K.J., Pickering, N.B., 1994. Modeling photosynthesis of row crop canopies. HortScience 29 (12), 1423–1434.

Boote, K.J., Jones, J.W., Hoogenboom, G., Pickering, N.B., 1998. The CROPGRO model for grain legumes. In: Tsuji, G.Y., Hoogenboom, G., Thornton, P.K. (Eds.), Understanding options for agricultural production. Kluwer Academic Publishers, London, pp. 99–128.

Boote, K.J., Sau, F., Hoogenboom, G., Jones, J.W., 2008. Experience with water balance, evapotranspiration, and predictions of water stress effects in the CROPGRO model. Response of Crops to Limited Water: Understanding and Modeling Water Stress Effects on Plant Growth Processes, pp 59–103. Volume 1 of Advances in Agricultural Systems Modeling. ASA-CSSA-SSSA, Madison, WI.

Boote, K.J., J.W. Jones, and G. Hoogenboom. 2021. Incorporating realistic trait physiology into crop growth models to support genetic improvement. in silico Plants. (Accepted for Publication).

Brisson, N., Seguin, B., Bertuzzi, P., 1992. Agrometeorological soil water balance for crop simulation models. Agric. For. Meteorol. 59 (3–4), 267–287.

Campelo, G.J., Kiihl, R.A. S., Almeida, L.A., 1998. Soybean: development for low latitude regions. Teresina: Embrapa Meio-Norte, 36.

Candogan, B.N., Sincik, M., Buyukcangaz, H., Demirtas, C., Goksoy, A.T., Yazgan, S., 2013. Yield, quality and crop water stress index relationships for deficit-irrigated soybean [*Glycine max* (L.) Merr.] in sub-humid climatic conditions. Agric. Water Manag. 118, 113–121.

Carpentieri-Pípolo, V., Almeida, L.A.D., Kiihl, R.A.D.S., 2002. Inheritance of a long juvenile period under short-day conditions in soybean. Genet. Mol. Biol. 25 (4), 463–469.

Corbeels, M., Chirat, G., Messad, S., Thierfelder, C., 2016. Performance and sensitivity of the DSSAT crop growth model in simulating maize yield under conservation agriculture. Eur. J. Agron. 76, 41–53.

Dexter, A.R., 2004. Soil physical quality: Part I. Theory, effects of soil texture, density, and organic matter, and effects on root growth. Geoderma 120 (3–4), 201–214.

Erbs, D.G., Klein, S.A., Duffie, J.A., 1982. Estimation of the diffuse radiation fraction for hourly, daily and monthly-average global radiation. Sol. Energy 28 (4), 293–302.

Fehr, W.R., Caviness, C.E., 1977. Stages of Soybean Development. Iowa State University, Ames.

Gijsman, A.J., Hoogenboom, G., Parton, W.J., Kerridge, P.C., 2002. Modifying DSSAT crop models for low-input agricultural systems using a soil organic matter–residue module from CENTURY. Agron. J. 94 (3), 462–474.

Gimenes, F.H.S., 2016. Propriedades de retenção e condução da água no solo determinadas sob condições de campo. Universidade de São Paulo, Piracicaba.

Gonçalves, A.O., Silva, E.H.F.M., Gasparotto, L.G., Mantelatto, J.R., Carmo, S., Fattori Júnior, I.M., Marin, F.R., 2020. Improving indirect measurements of the leaf area index using canopy height. Pesq. Agropec. Bras. 55, 1–9.

Grimm, S.S., Jones, J.W., Boote, K.J., Hesketh, J.D., 1993. Parameter estimation for predicting flowering date of soybean cultivars. Crop Sci. 33 (1), 137–144.

Grimm, S.S., Jones, J.W., Boote, K.J., Herzog, D.C., 1994. Modeling the occurrence of reproductive stages after flowering for four soybean cultivars. Agron. J. 86 (1), 31–38.

Heinemann, A.B., Hoogenboom, G., Georgiev, G.A., de Faria, R.T., Frizzone, J.A., 2000. Center pivot irrigation management optimization of dry beans in humid areas. Trans. ASAE 43 (6), 1507–1516.

Hoogenboom, G., C.H. Porter, V. Shelia, K.J. Boote, U. Singh, J.W. White, L.A. Hunt, R. Ogoshi, J.I. Lizaso, J. Koo, S. Asseng, A. Singels, L.P. Moreno, Jones, J.W., 2019b. Decision Support System for Agrotechnology Transfer (DSSAT) Version 4.7 (⟨www.DSSAT.net⟩). DSSAT Foundation, Gainesville, Florida, USA.

Hoogenboom, G., J.W. Jones, K.J. Boote., 1991. A decision support system for prediction of crop yield, evapotranspiration, and irrigation management. p. 198–204. In: [W. F. Ritter, editor] Irrigation and Drainage: Proceedings of the 1991 National Conference. American Society of Civil Engineers, New York, New York.

Hoogenboom, G., Porter, C.H., Boote, K.J., Shelia, V., Wilkens, P.W., Singh, U., White, J. W., Asseng, S., Lizaso, J.I., Moreno, L.P., Pavan, W., Ogoshi, R., Hunt, L.A., Tsuji, G. Y., Jones, J.W., 2019a. The DSSAT crop modeling ecosystem. In: Boote, K.J. (Ed.), Advances in Crop Modeling for a Sustainable Agriculture. Burleigh Dodds Science Publishing, Cambridge, United Kingdom, pp. 173–216.

Jones, J.W., Keating, B.A., Porter, C.H., 2001. Approaches to modular model development. Agric. Syst. 70 (2–3), 421–443.

Jones, J.W., Hoogenboom, G., Porter, C.H., Boote, K.J., Batchelor, W.D., Hunt, L.A., Wilkens, P.W., Singh, U., Gijsman, A.J., Ritchie, J.T., 2003. The DSSAT cropping system model. Eur. J. Agron. 18 (3–4), 235–265.

Jones, J.W., Boote, K.J., Hoogenboom, G., Jagtap, S.S., Wilkerson, G. G., 1989. SOYGRO V5. 42, Soybean crop growth simulation model. User's guide. Florida Agricultural Experiment Station Journal, 8304, 83.

Kamienski, C., Soininen, J.P., Taumberger, M., Dantas, R., Toscano, A., Salmon Cinotti, T., Maia, R.F., Torre Neto, A., 2019. Smart water management platform: Iot-based precision irrigation for agriculture. Sens. (Basel, Switz.) 19 (2), 276.

Kim, J., Schultz HK, S., 2020. Advances and improvements in modeling plant processes. In Advances in crop modelling for a sustainable agriculture (pp. 3–43). Dublin: Burleigh Dodds Science.

Kimball, B.A., Bellamy, L.A., 1986. Generation of diurnal solar radiation, temperature, and humidity patterns. Energy Agric. 5 (3), 185–197.

Köppen, W.P., 1931. Grundriss der Klimakunde: 2. verb. Aufl. der Klimate der Erde. W. de Gruyter.

Liu, H.L., Yang, J.Y., Tan, C.S., Drury, C.F., Reynolds, W.D., Zhang, T.Q., Bai, J.J., He, P., Hoogenboom, G., 2011. Simulating water content, crop yield and nitrate-N loss under free and controlled tile drainage with subsurface irrigation using the DSSAT model. Agric. Water Manag. 98 (6), 1105–1111.

Loague, K., Green, R.E., 1991. Statistical and graphical methods for evaluating solute transport models: overview and application. J. Contam. Hydrol. 7 (1–2), 51–73.

Marin, F.R., Jones, J.W., Royce, F., Suguitani, C., Donzeli, J.L., Filho, W.J.P., Nassif, D.S., 2011. Parameterization and evaluation of predictions of DSSAT/CANEGRO for Brazilian sugarcane. Agron. J. 103 (2), 304–315.

Marin, F.R., Angelocci, L.R., Nassif, D.S., Vianna, M.S., Pilau, F.G., da Silva, E.H., Sobenko, L.R., Goncalves, A.O., Pereira, R.A., Carvalho, K.S., 2019. Revisiting the crop coefficient–reference evapotranspiration procedure for improving irrigation management. Theor. Appl. Climatol. 138 (3–4), 1785–1793.

Melo, F. de B., de Andrade Junior, A.S., Pessoa, B.L. de O., 2014. Levantamento, zoneamento e mapeamento pedológico detalhado da área experimental da Embrapa Meio-Norte em Teresina, PI. Teresina: Embrapa Meio-Norte-Documentos.

Multsch, S., Krol, M.S., Pahlow, M., Assunção, A.L.C., Barretto, A.G.O.P., de Jong van Lier, Q., Breuer, L., 2020. Assessment of potential implications of agricultural irrigation policy on surface water scarcity in Brazil. Hydrol. Earth Syst. Sci. 24 (1), 307–324.

Nieuwolt, S., 1989. Estimating the agricultural risks of tropical rainfall. Agric. For. Meteorol. 45 (3–4), 251–263.

Nijbroek, R., Hoogenboom, G., Jones, J.W., 2003. Optimal irrigation strategy for a spatially variable soybean field: a modeling approach. Agric. Syst. 76 (1), 359–377.

Parton, W.J., Logan, J.A., 1981. A model for diurnal variation in soil and air temperature. Agric. Meteorol. 23, 205–216.

Parton, W.J., McKeown, B., Kirchner, V., Ojima, D., 1992. Century users manual. Natural Resource Ecology Laboratory. Colorado State University, Fort Collins.

Pereira, A.R., Nova, N.A.V., 1992. Analysis of the Priestley-Taylor parameter. Agric. For. Meteorol. 61 (1–2), 1–9.

Pivetta, L.A., Castoldi, G., Santos, G.P.D., Rosolem, C.A., 2011. Soybean root growth and activity as affected by the production system. Pesqui. Agropecuária Bras. 46 (11), 1547–1554.

Porter, C.H., Jones, J.W., Hoogenboom, G., Wilkens, P.W., Ritchie, J.T., Pickering, N.B., Boote, K., Baer, B., 2004. DSSAT v4 soil water balance module. Decis. Support Syst. Agrotechnol. Transf. Version 4, 1–23.

Porter, C.H., Jones, J.W., Adiku, S., Gijsman, A.J., Gargiulo, O., Naab, J.B., 2010. Modeling organic carbon and carbon-mediated soil processes in DSSAT v4. 5. Oper. Res. 10 (3), 247–278.

Priestley, C.H.B., Taylor, R.J., 1972. On the assessment of surface heat flux and evaporation using large-scale parameters. Mon. Weather Rev. 100 (2), 81–92.

Qubaja, R., Amer, M., Tatarinov, F., Rotenberg, E., Preisler, Y., Sprintsin, M., Yakir, D., 2020. Partitioning evapotranspiration and its long-term evolution in a dry pine forest using measurement-based estimates of soil evaporation. Agric. For. Meteorol. 281, 1–10.

Richetti, J., Boote, K.J., Hoogenboom, G., Judge, J., Johann, J.A., Uribe-Opazo, M.A., 2019. Remotely sensed vegetation index and LAI for parameter determination of the CSM-CROPGRO-Soybean model when in situ data are not available. Int. J. Appl. Earth Obs. Geoinf. 79, 110–115.

Ritchie, J.T., 1981. Water dynamics in the soil-plant-atmosphere system. Plant Soil 58, 81–96.

Ritchie, J.T., 1985. A user-orientated model of the soil water balance in wheat. In Wheat Growth and Modelling. Springer, Boston, pp. 293–305.

Ritchie, J.T., 1998. Soil water balance and plant water stress. In Understanding Options for Agricultural Production London. Kluwer Academic Publishers, pp. 41–54.

Rosa, M.F., Bonham, C.A., Dempewolf, J., Arakwiye, B., 2017. An integrated approach to monitoring ecosystem services and agriculture: implications for sustainable agricultural intensification in Rwanda. Environ. Monit. Assess. 189 (1), 15.
Salmerón, M., Purcell, L.C., 2016. Simplifying the prediction of phenology with the DSSAT-CROPGRO-soybean model based on relative maturity group and determinacy. Agric. Syst. 148, 178–187.
Sau, F., Boote, K.J., Ruíz-Nogueira, B., 1999. Evaluation and improvement of CROPGRO-soybean model for a cool environment in Galicia, northwest Spain. Field Crops Res. 61 (3), 273–291.
Sau, F., Boote, K.J., Bostick, W.M., Jones, J.W., Mínguez, M.I., 2004. Testing and improving evapotranspiration and soil water balance of the DSSAT crop models. Agron. J. 96 (5), 1243–1257.
Shelia, V., Šimůnek, J., Boote, K., Hoogenbooom, G., 2018. Coupling DSSAT and HYDRUS-1D for simulations of soil water dynamics in the soil-plant-atmosphere system. J. Hydrol. Hydromech. 66 (2), 232–245.
Silva, E.H.F.M., Gonçalves, A.O., Pereira, R.A., Júnior, I.M.F., Sobenko, L.R., Marin, F.R., 2019. Soybean irrigation requirements and canopy-atmosphere coupling in Southern Brazil. Agric. Water Manag. 218, 1–7.
Soldevilla-Martinez, M., Quemada, M., López-Urrea, R., Munoz-Carpena, R., Lizaso, J.I., 2014. Soil water balance: comparing two simulation models of different levels of complexity with lysimeter observations. Agric. Water Manag. 139, 53–63.
Soltani, A., Sinclair, T.R., 2012. Modeling physiology of crop development, growth and yield. Podicherry. CABi.
Souza, P.I., Egli, D.B., Bruening, W.P., 1997. Water stress during seed filling and leaf senescence in soybean. Agron. J. 89 (5), 807–812.
Spitters, C.J.T., 1986. Separating the diffuse and direct component of global radiation and its implications for modeling canopy photosynthesis Part II. Calculation of canopy photosynthesis. Agric. For. Meteorol. 38 (1–3), 231–242.
Spitters, C.J.T., Toussaint, H.A.J.M., Goudriaan, J., 1986. Separating the diffuse and direct component of global radiation and its implications for modeling canopy photosynthesis Part I. Components of incoming radiation. Agric. For. Meteorol. 38 (1–3), 217–229.
Suleiman, A.A., Ritchie, J.T., 2003. Modeling soil water redistribution during second-stage evaporation. Soil Sci. Soc. Am. J. 67 (2), 377–386.
Thornton, P.K., Hoogenboom, G., 1994. A computer program to analyze single-season crop model outputs. Agron. J. 86 (5), 860–868.
Topp, G.C., Davis, J.L., Annan, A.P., 1980. Electromagnetic determination of soil water content: measurements in coaxial transmission lines. Water Resour. Res. 16 (3), 574–582.
Tsuji, G.Y., Hoogenboom, G., Thornton, P.K., 1998. Understanding options for agricultural production. Systems Approaches for Sustainable Agricultural Development. Kluwer Academic Publishers, Dordrecht, the Netherlands, p. 400.
Uryasev, O., Gijsman, A.J., Jones, J.W., Hoogenboom, G., Wilkens, P.W., Porter, C.H., 2004. DSSAT v4 Soil data editing program [Sbuild]. Decis. Support Syst. Agrotechnol. Transf. Version 4, 2–14.
Valentín, F., Nortes, P.A., Domínguez, A., Sánchez, J.M., Intrigliolo, D.S., Alarcón, J.J., López-Urrea, R., 2020. Comparing evapotranspiration and yield performance of maize under sprinkler, superficial and subsurface drip irrigation in a semi-arid environment. Irrig. Sci. 38 (1), 105–115.
Viana, J.S., Gonçalves, E.P., Silva, A.C., Matos, V.P., 2013. Climatic conditions and production of soybean in Northeastern Brazil. A Comprehensive Survey of International Soybean Research-Genetics, Physiology, Agronomy and Nitrogen Relationships. InTech,, pp. 377–392.
Villa Nova, N.A., Pereira, A.B., 2006. Ajuste do método de Priestley-Taylor às condições climáticas locais. Eng. Agríc. 26 (2), 395–405.
Wilkerson, G.G., Jones, J.W., Boote, K.J., Ingram, K.T., Mishoe, J.W., 1983. Modeling soybean growth for crop management. Trans. ASAE 26 (1), 63–0073.
Williams, J.R., 1991. Runoff and water erosion. In Modeling Plant and Soil Systems. ASA-CSSA-SSSA, Wisconsin, pp. 439–455.
Willmott, C.J., Ackleson, S.G., Davis, R.E., Feddema, J.J., Klink, K.M., Legates, D.R., O'Donnell, J., Rowe, C.M., 1985. Statistics for the evaluation and comparison of models. J. Geophys. Res. Oceans 90 (C5), 8995–9005.
Yang, J.M., Yang, J.Y., Liu, S., Hoogenboom, G., 2014. An evaluation of the statistical methods for testing the performance of crop models with observed data. Agric. Syst. 127, 81–89.
Zaffar, M., Sheng-Gao, L.U., 2015. Pore size distribution of clayey soils and its correlation with soil organic matter. Pedosphere 25 (2), 240–249.
Zhou, H., Zhi Zhao, W., 2019. Modeling soil water balance and irrigation strategies in a flood-irrigated wheat-maize rotation system. A case in dry climate, China. Agric. Water Manag. 221, 286–302.